Preparation of Ca- and Na-Modified Activated Clay as a Promising Heterogeneous Catalyst for Biodiesel Production via Transesterification

Yue Wang [1] , Yaseen Muhammad [2] , Sishan Yu [1], Tian Fu [1], Kun Liu [3], Zhangfa Tong [3], Xueling Hu [4,*] and Hanbing Zhang [1,3,*]

1 School of Resources, Environment and Materials, Guangxi University, Nanning 530004, China; wyue_131@163.com (Y.W.); yusan1498122449@outlook.com (S.Y.); ft18241868138@163.com (T.F.)
2 Institute of Chemical Sciences, University of Peshawar, Peshawar 25120, Pakistan; myyousafzai@gmail.com
3 Guangxi Key Laboratory of Petrochemical Resource Processing and Process Intensification Technology, School of Chemistry and Chemical Engineering, Guangxi University, Nanning 530004, China; chentu189@163.com (K.L.); zftong@gxu.edu.cn (Z.T.)
4 Institute of Biomanufacturing Technology, Guangxi Institute of Industrial Technology (GIIT), Nanning 530200, China
* Correspondence: gxhxling@sina.com (X.H.); coldicezhang0771@163.com (H.Z.); Tel.: +86-137-0787-5059 (X.H.); +86-130-7777-6827 (H.Z.)

Abstract: For efficient biodiesel production, an acid-activated clay (AC) modified by calcium hydroxide and sodium hydroxide (CaNa/AC) was prepared as a catalyst. CaNa/AC and Na/AC were characterized by Hammett indicators, CO_2-TPD, FT-IR, XRD, and N_2 adsorption techniques. The influence of catalyst dose, reaction temperature, methanol/oil molar ratio, and reaction time on the transesterification of Jatropha oil was studied. Due to the introduction of calcium, CaNa/AC displayed a higher activity and stability, thereby achieving an oil conversion of 97% under the optimal reaction conditions and maintaining over 80% activity after five successive reuses. The reaction was accelerated as the temperature rose, and the apparent activation energy of CaNa/AC was 75.6 kJ·mol^{-1}. The enhanced biodiesel production by CaNa/AC was ascribed to the increase in active sites and higher basic strength. This study presents a facile and practical method for producing biodiesel on large-scale operation.

Keywords: biodiesel; Jatropha oil; transesterification; modified clay; heterogeneous catalyst

1. Introduction

Biodiesel, which contains fatty acid alkyl esters and generally exists in the form of fatty acid methyl esters (FAME), is an attractive alternative fuel due to its superior properties including biodegradability, renewability, and low toxicity. Biodiesel production and consumption have rapidly expanded in recent years because of its positive environmental effects [1,2]. The most common method for obtaining biodiesel is the methanolysis of highly refined oil in the presence of homogeneous alkaline catalysts such as NaOH, KOH, CH_3ONa, and CH_3OK [3,4]. These homogeneous-basic catalysts, on the other hand, cannot be recovered or regenerated after the reaction and should be neutralized with acid or removed with a substantial volume of hot water, raising overall biodiesel production costs and causing significant environmental damage. Compared with homogeneous-based catalysts, heterogeneous-based catalysts are easier to be separated from liquid products, have improved selectivity, and can be regenerated and reused, thus decreasing the challenges associated with their disposal and minimizing process costs [5]. In certain cases, heterogeneous catalysis allows for a switch in reactivity, enabling the development of new and more beneficial synthetic methods [6]. Therefore, it is imperative to develop promising methods for biodiesel production utilizing heterogeneous base catalysts.

Salts or hydroxides of alkali metals (as active precursors) are generally more active than acids in transesterification [7], and frequently imported into suitable support materials such as zirconium dioxide [8], magnesia [9,10], silica [11], and zeolites [12,13] for the preparation of heterogeneous base catalysts. However, these catalysts require costly supports or high-temperature thermal treatments, which incur higher catalyst production costs and offset the economic and environmental advantages of biodiesel production. Therefore, the application of these heterogeneous-based catalysts in realistic large-scale biodiesel production is still limited. Fortunately, clay-based or modified clay-based catalysts have attracted the attention of researchers looking for low-cost raw materials. Some clay catalysts such as NaOH-activation kaolin clay [14], KOH-treated bentonite, and KF-modified smectite clay [15] have been reported for biodiesel production on the laboratory scale via the transesterification of vegetable oil in excess methanol. However, they also have some inherent shortcomings such as the requirement of high-temperature thermal treatment and the use of the toxic precursor (KF). Based on the above discussions, sufficient research focused on the preparation of an efficient and affordable catalyst for biodiesel production is very necessary.

Herein, we report the synthesis of an economical and eco-friendly acid-activated clay (AC) catalyst by treating the local clay with a waste acid recycling method, and the as-prepared AC catalyst was further applied in biodiesel production under ambient reaction conditions. This can effectively and ingeniously maximize the resource utilization of waste and low-cost clay. Due to the main component of natural clay being montmorillonite and quartz contained in local clay, AC possessed the characteristics of acid-activated montmorillonite, such as high specific surface area, surface acidity, and mesoporous structure [16–18]. Therefore, AC has been widely reported in various catalytic reactions [19–21] and as a catalyst support [22,23]. Notably, the information about solid base catalysts derived from AC in the production of biodiesel is scarce.

In this study, AC was successively modified by calcium hydroxide and sodium hydroxide to prepare a novel Ca- and Na-modified AC-based clay (CaNa/AC) catalyst and then applied in biodiesel production from Jatropha oil. Na-modified AC (Na/AC) as the reference catalysts was also prepared for comparison. The as-prepared catalysts were characterized by a series of characterizations including Hammett indicators, CO_2-temperature program desorption (CO_2-TPD), Fourier transform infrared (FT-IR) spectroscopy, X-ray diffraction (XRD), and N_2 adsorption techniques. Furthermore, the reaction conditions of the transesterification on CaNa/AC were optimized and the reusability of catalysts was investigated. Additionally, a plausible reaction mechanism for biodiesel production was elaborated in detail on the basis of characterization results.

2. Materials and Methods

2.1. Materials and Reagents

Bentonite was collected from Guangxi Province, China. AC was produced by acidifying bentonite with waste sulfuric acid. The total amount of acid centers obtained by acidifying bentonite and the number of Brønsted and Lewis acid sites would be influenced by the type of acid chosen for the acidification process, the concentration of the acid, and other process conditions [24], and the activation method for AC was referenced to a previous study [25]. The acidity of samples was calculated by a Nicolet 6700 FT-IR model, Thermo Scientific, and standard acid-base titration, and the result was 1.56 mmol·g^{-1} [26].

Jatropha oil was purchased from Jiangsu Province, China. The acid value (AV) and saponification value (SV) of the refined Jatropha oil were 0.23 mg KOH·g^{-1} and 188.4 mg KOH·g^{-1}, as calculated following the Chinese national standard GB/T 5530-2005 and 5534-2008, respectively. The main fatty acids of the Jatropha oil were identified and quantified as follows: palmitic acid (C16:0), 14.9%; oleic acid (C18:2), 40.9%; linoleic acid (C18:1), 38.1%; and stearic acid (C18:0), 6.1%. CaO and NaOH were of analytical grade and obtained commercially.

2.2. Preparation of Catalysts

AC was prepared by a traditional wet method. An amount of 50 g bentonite was taken in a beaker, mixed with 175 mL of H_2SO_4, and heated at 363 K for 4 h in a water bath with a magnetic stirrer. The concentration of H_2SO_4 solution was varied between 16% and 24% by mass. After acid treatment, each sample was filtered under vacuum and the precipitate was washed with distilled water until the pH of the filtrate was above 5.0. Then, AC was dried at 378 K for 4 h, ground to a powder, and stored in the desiccator.

The steps for the modification of AC with calcium hydroxide were as follows: Under 200 $r \cdot min^{-1}$ stirring, 100 g of AC was suspended in 300 mL of deionized water and heated to 343 K, and calcium hydroxide emulsion was slowly added. The acidity of the system was measured using a precision pH meter, and the monolayer loading of AC with calcium hydroxide was completed at 0.3 mol contents of calcium hydroxide. The amount of calcium hydroxide needed for AC modification was calculated to be 16.8 g of CaO per 100 g of AC.

AC was first modified with calcium hydroxide with the goal of sheltering the acid center of AC and avoiding excessive corrosion of the montmorillonite flake layer by the subsequent loading of sodium hydroxide. Details of the preparation are as follows: 100 g of AC was evenly dispersed in 300 mL of deionized water at 343 K under continuous stirring. Then, $Ca(OH)_2$ emulsion (the mixture of 16.8 g of CaO and 20 mL of deionized water) was added into the mixture slowly. After continuously stirring for 1 h, an 80 mL NaOH solution (11.3 mol/L) was dropwise added into the above suspension. Then, the slurry was stirred for 2 h at 343 K followed by filtering it. The obtained filtrate was reserved for later use in the regeneration of the catalysts. The filter cake was dried at 473 K for 2 h, crushed into power, and screened through a 200-mesh sieve. The powder (CaNa/AC) was kept in an inert environment. Furthermore, according to the above method, Ca/AC and Na/AC composites were prepared via AC modified by $Ca(OH)_2$ and NaOH, respectively, which served as reference materials.

2.3. Characterizations

The base strengths (H_) of the samples were determined using Hammett indicators, including bromothymol blue (H_ = 7.2), phenolphthalein (H_ = 9.8), indigo carmine (H_ = 12.2), 2,4-dinitroaniline (H_ = 15.0), and 4-nitroaniline (H_ = 18.4) [27]. The basicity of the catalysts was measured by Hammett indicators in triplicate readings, and the average values were reported along with the standard deviation [28].

The properties of the samples were determined by CO_2-TPD. Prior to CO_2 adsorption, 50 mg of Ca/AC and Na/AC was pretreated under a He flow (20 $mL \cdot min^{-1}$) at 473 K for 30 min. Then, after cooling down to 373 K, CO_2 was pumped into the sample for 90 min. After that, physically adsorbed CO_2 was removed by He flow purging (30 $mL \cdot min^{-1}$) at 373 K for 2 h. Ca/AC and Na/AC were then heated to 1173 K with a ramp of 283 $K \cdot min^{-1}$. Moreover, the content of desorbed CO_2 was detected by a gas chromatograph (GC) equipped with a thermal conductivity detector (TCD).

The FT-IR study was performed on a Perkin-Elmer Spectrum GX system with a standard mid-IR DTGS detector in the wavenumber range of 400–4000 cm^{-1}. XRD patterns were collected on a D/max 2500 V X-ray diffractometer (Japan), and the crystalline phases of samples were identified by referencing the JCPDS card library. The specific surface areas (SSA) and pore size distributions of the samples were determined using a Quantachrome NOVA 1200e piece of volumetric gas adsorption equipment (USA). The samples were degassed for 2 h under vacuum at 473 K before being tested at 77 K with nitrogen as an adsorbate. The Brunauer–Emmett–Teller (BET) model was adopted to compute SSA, and the Barrett–Joyner–Halenda (BJH) model was used to determine the pore size distribution and pore volume.

2.4. Catalytic Activity Test and Optimization of Transesterification Conditions

In the transesterification process, the performance of the produced catalysts was evaluated. The reactions were carried out at 338 K for 3 h with a 5 wt.% catalyst amount

and a methanol/oil molar ratio of 10:1. The transesterification processes were carried out in a three-neck reaction flask with a magnetic stirrer and a water-cooled condenser. The flask was charged with 100 g of Jatropha oil and then heated in the water bath to the desired temperature. Then, methanol and catalyst were added to the oil, and the reaction mixture was agitated at 600 rpm. Centrifugation was used to separate the biodiesel phase from the catalyst and glycerol after the end of the transesterification process. Finally, rotary evaporation was used to eliminate any residual methanol in the biodiesel phase. To determine the FAME content of the product, the obtained biodiesel product was analyzed on an Agilent 7820 GC by using an internal standard method. The previously mentioned techniques were used to determine the conversion of oil to biodiesel [29]. The content in FAME of the biodiesel sample was determined using gas chromatography (GC, Agilent 7820, FID) following the European regulated procedure EN14103. In the work, biodiesel samples were analyzed by GC to determine the FAME content of the product. The GC was equipped with an HP-1 capillary with dimensions of 30 m × 0.32 nm × 0.25 μm. Sample volumes were 1.0 μL, the carrier gas was nitrogen, and the GC sample was separated in a constant flow mode with a flow rate of 4.0 mL·min^{-1}. A split injector was used with a split ratio of 40 and a temperature of 553 K. The oven temperature was initially held at 423 K, then elevated to 473 K at a rate of 293 K·min^{-1} and further elevated to 503 K at a rate of 274.8 K·min^{-1}, held for 1 min, and finally raised to 533 K at a rate of 283 K·min^{-1}. The total run time was 26 min. The internal standard was methyl tridecanoate. To investigate the optimum conditions for the transesterification of Jatropha oil, CaNa/AC was applied to conduct a series of transesterification reactions using various catalyst amounts (1–5 wt.%) and temperatures (323–343 K) at different methanol/oil molar ratios (6:1–14:1) and times (1–5 h). Each transesterification reaction was performed in triplicate, and the average values were reported.

2.5. Kinetics Experiment

For kinetics studies, the transesterification reactions described above were performed using CaNa/AC at 323, 328, 333, and 338 K, respectively. During the reactions, 1 mL samples were collected at 10, 20, 30, 60, 90, 120, 180, 240, 300, and 360 min time intervals, and then analyzed by GC to determine the conversion efficiency.

2.6. Catalyst Recycling

For recycling performance evaluation, at the end of the transesterification reaction, the catalyst was filtered from the reaction mixture and washed 2–3 times with 10 mL of n-hexane. The deactivated catalyst was regenerated by treating in the filtrate reserved from the preparation process of catalyst for 2 h, filtered, and dried at 473 K. The regenerated catalyst was applied for the next run under identical reaction conditions.

3. Results

3.1. Base Strength and Basicity

The results of the base strength and basicity of AC, Ca/AC, Na/AC, and CaNa/AC are shown in Table 1, which suggested that AC was not basic. However, Ca/AC was alkalescent with the basic strength of H_ = 7.2~9.8, indicating that Ca(OH)$_2$ neutralized most of the acid sites in AC and replaced them with conjugated basic sites during the modification process. Ca/AC exhibited inferior catalytic activity in the transesterification reaction due to its weak H_ [30,31]. Compared with Ca/AC, CaNa/AC presented a higher basic strength and basicity, which indicated that the amount of stronger basic sites increased with the introduction of Na, thereby resulting in an improvement in catalytic activity. Moreover, the oil conversion of Na/AC (58.6%) was larger than that of Ca/AC, which is due to the fact that the introduction of NaOH increased the basicity, which contributed to the higher oil conversion. The synergistic effect of both sodium and calcium attributed to the highest base strength of CaNa/AC.

Table 1. Basic strength, basicity, and catalytic activity of AC, Ca/AC, Na/AC, and CaNa/AC.

Sample	Basic Strength (H_)	Basicity (mmol of HCl·g^{-1})	Conversion (%)
AC	H_ < 7.2	-	-
Ca/AC	7.2 < H_ < 9.8	1.4	7.3
Na/AC	12.2 < H_ < 15.0	3.3	58.6
CaNa/AC	15.0 < H_ < 18.4	5.0	81.3

CaNa/AC at 5 wt.% catalyst amount, methanol/oil molar ratio of 10:1, and 338 K for 3 h with 600 rpm.

3.2. CO_2-TPD Analysis

In order to further verify the effect of Na on the basicity of CaNa/AC, the CO_2-TPD of Ca/AC and CaNa/AC was performed, and the corresponding results are shown in Figure 1a. Four CO_2 desorption peaks were observed in the spectrum of Ca/AC where the two peaks at 503 K and 853 K could be attributed to the weak basic sites and moderate basic sites, respectively; while the other two low-intensity peaks with intensity maxima at 941 K and 998 K, respectively, corresponded to strong basic sites [32]. For Na/AC, the desorption peak (954–990 K) could be attributed to the moderate basic sites, and for CaNa/AC, the desorption peaks shifted to a higher temperature. Moreover, the intensity of the peaks of strong basic sites (923–1053 K) was substantially higher than that of Ca/AC, which indicated that the incorporation of Na ions increased the basicity of the material and the number of strong basic sites, resulting in enhanced catalytic activity.
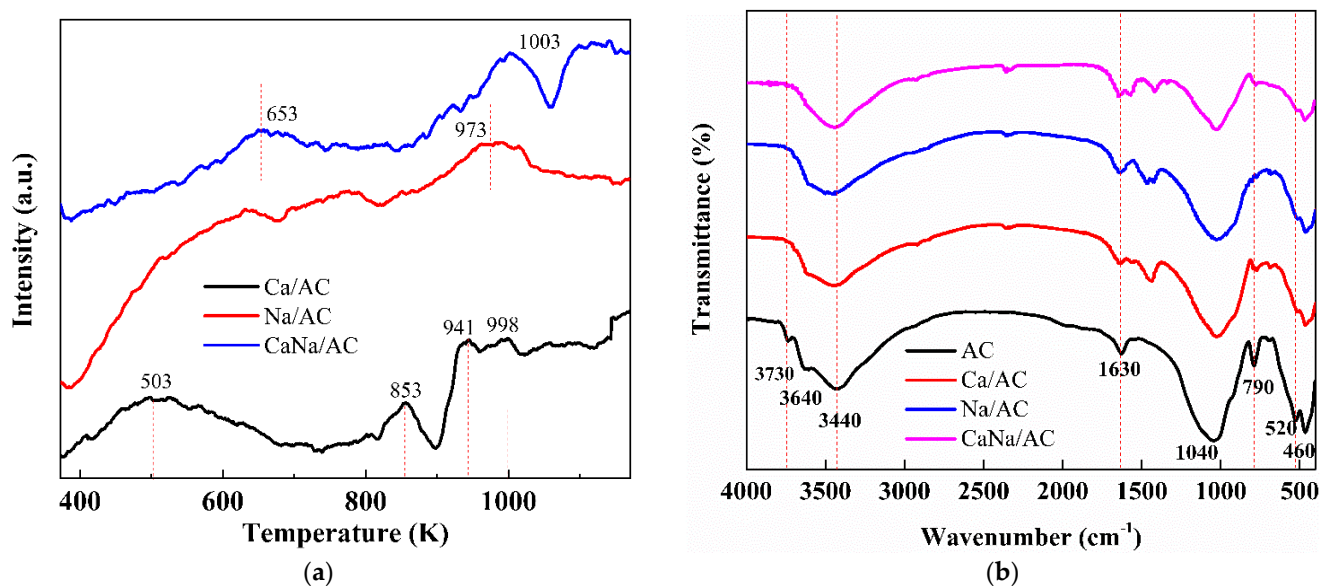

Figure 1. (**a**) CO_2-TPD profiles of Ca/AC, Na/AC, and CaNa/AC; (**b**) FT-IR spectra of AC, CA/AC, Na/AC, and CaNa/AC.

3.3. FT-IR Analysis

FT-IR spectroscopy is effectively applied to study the chemical composition of materials in terms of functional group characterization [33,34]. All FT-IR results of samples are displayed in Figure 1b. In the spectrum of Ca/AC, the band at 3730 cm^{-1} (Si–OH) was almost absent due to the fact that Brønsted acid sites of AC were neutralized by Ca(OH)$_2$. Furthermore, in the spectra of the three modified samples, new peaks attributable to M–OH (M = Ca, Na) appeared at 1500–1400 cm^{-1}, which could be ascribed to the intense interactions of water molecules with the cations [35]. CaNa/AC and Na/AC bands at 1040 cm^{-1} (Si–O–Si) shifted to a lower frequency (red-shifted), indicating the generation of stronger basic sites in the samples, which is conducive to enhancing the catalytic activity [36]. However, due to the intense base solution erosion, the absence of the two peaks at 3730 cm^{-1} and 3640 cm^{-1} and the significant decrease in the intensity of the peak at 1040 cm^{-1} in the

spectrum of Na/AC suggested the obvious degradation of the mineral structure [37,38]. In addition, the characteristic montmorillonite bands at 1040 cm^{-1} and 3640 cm^{-1} suggested that the montmorillonite structure of CaNa/AC was more intact than that of Na/AC because of the addition of Ca, which is beneficial for enhancing the recycling performance of the catalyst.

3.4. XRD Analysis

The XRD patterns of as-prepared AC, Ca/AC, Na/AC, and CaNa/AC are shown in Figure 2a to clarify the crystallinity and crystal phase of the samples [39,40]. The reflection within the diffraction peaks of AC corresponded to the typical phases of montmorillonite and quartz [41]. In comparison to AC diffraction peaks, two peaks at 27.9° and 29.5° of the Ca/AC pattern could correspond to anorthite and montmorillonite, respectively [42,43]. The formation of these two peaks was attributed to the interaction between Ca(OH)$_2$ and AC acid sites, which indicated the successful introduction of calcium ions into the AC framework, the decrease in acid sites, and the production of weakly basic sites in the clay platelets. For Na/AC, the quartz characteristic peaks were mostly intact. On the contrary, the intensity of its montmorillonite peaks significantly decreased, especially at $2\theta = 5.8°$ and 19.7°, which suggested that NaOH directly reacted with the montmorillonite phase due to the surface acidity of AC, destroying its crystallinity. This was consistent with the FT-IR result for Na/AC, which showed a dramatic drop in the band at 1040 cm^{-1}. In the XRD pattern of CaNa/AC, the intensity of the characteristic peaks belonging to quartz decreased, while the major peaks corresponding to montmorillonite remained relatively high in intensity, which indicated that CaNa/AC still retained the montmorillonite mineral structure. Therefore, it could be deduced that the addition of Ca contributed to reinforcing the stability of the catalyst, which is beneficial for reuse in biodiesel production. In addition, the 001 plane (the characteristic reflection) shifted to the larger angles in CaNa/AC and Na/AC catalysts, indicating a decrease in montmorillonite interlamellar distance caused by the introduction of sodium cations with reduced hydration energy. Furthermore, several new peaks of sodium compounds were generated in the XRD pattern of CaNa/AC. The characteristic peaks of sodium species with low intensity could be covered by the montmorillonite peaks. However, there were no new peaks in Na/AC, suggesting that the sodium ions were only adsorbed on the surface, which exerted a negative impact on the activity and stability of Na/AC.
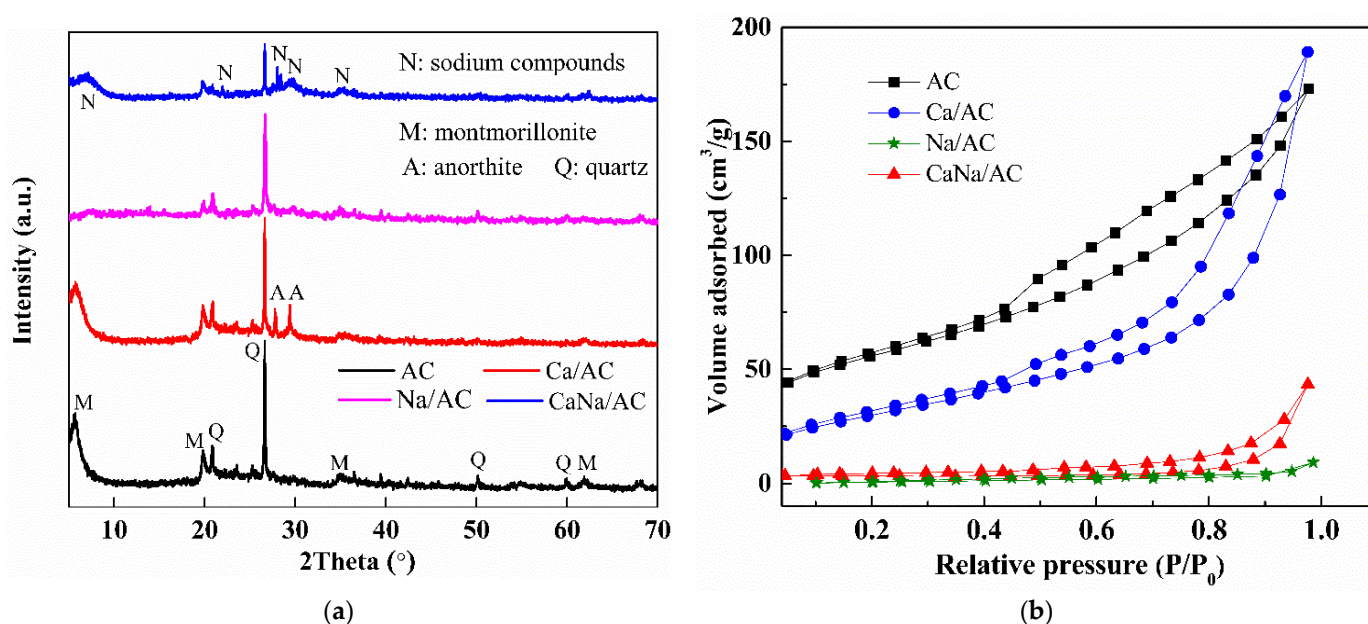

Figure 2. (**a**) The XRD patterns and (**b**) nitrogen adsorption–desorption isotherms of AC, CA/AC, Na/AC, and CaNa/AC.

3.5. BET Analysis

The BET surface areas, average pore diameter, and total pore volume of different samples were obtained by utilizing the nitrogen adsorption/desorption isotherms (Figure 2b), and the corresponding results are summarized in Table 2. The average pore diameter of these samples was distributed in the range of 2–50 nm, suggesting their mesoporous nature according to the IUPAC classification [44]. The surface area of Ca/AC was smaller than that of AC, which indicated that the surface and pores of AC were partially covered after the modification [45]. There were obvious decreases in the surface area and porosity of CaNa/AC as compared to those of Ca/AC. However, this does not detrimentally affect the catalyst performance in the transesterification, as the introduction of sodium generates strong basic sites on the surface of CaNa/AC [46]. The activity of a solid alkali catalyst could be influenced not only by its surface structural properties but also by its alkali strength and amount of alkali, with the latter frequently having a larger effect [29]. The SSA, pore volume, and pore size of Na/AC were all smaller than those of the catalyst sample CaNa/AC, particularly the pore volume, because when NaOH was loaded directly onto AC, the strong base NaOH severely corroded the montmorillonite lamellae in AC, forming a denser structure that reduced the pore size and caused the material's pore volume to drop dramatically. This also verifies the conclusions of XRD and FT-IR analyses.

Table 2. Surface area, total pore volume, and average pore diameter of AC, Ca/AC, Na/AC, and CaNa/AC.

Sample	Surface Area $(m^2 \cdot g^{-1})$	Total Pore Volume $(cm^3 \cdot g^{-1})$	Average Pore Diameter (nm)
AC	138	0.27	6
Ca/AC	110	0.28	11
Na/AC	13	0.02	2
CaNa/AC	15	0.07	29

3.6. Influence of Reaction Conditions on the Transesterification

CaNa/AC was applied to investigate the optimum conditions for the transesterification of Jatropha oil. The initial conditions were set as: 10:1 methanol-to-oil molar ratio, 338 K reaction temperature, 3 h reaction duration, and 600 rpm stirring speed. As shown in Figure 3a, the conversion increased from 27% to 80% when the catalyst amount increased from 1.0 to 3.0 wt.%, which was attributed to the availability of more basic sites by a larger amount of catalyst, as well as an increase in the frequency of interaction between the reactants and catalyst. However, no significant changes to the conversion were observed when the catalyst amount was increased from 3.0 to 5.0 wt.%. As a result, the optimal 3.0 wt.% catalyst amount was selected for the next experiments.

Normally, the alkali-catalyzed transesterification of oil occurs at the boiling point of alcohol present in the reaction mixture [47–49]. In order to assess the influence of reaction temperature on the conversion, the transesterification was performed at 323, 328, 333, 338, and 343 K while other conditions were kept constant. As shown in Figure 3b, the conversion increased with increasing temperature from 323 to 338 K, and the maximum efficiency reached 80% at 338 K. As more energy was given for the reaction to proceed, a greater reaction temperature might reduce the viscosities of oils and raise the reaction rate [50,51]. Thus, the conversion could be improved with increasing reaction temperature. However, the conversion slightly decreased when the temperature was beyond 338 K, which could be due to the fact that the boiling point of methanol is 337.7 K at atmospheric pressure. In general, a very high reaction temperature accelerates the loss of methanol by vaporization, which consequently led to decreased conversion.
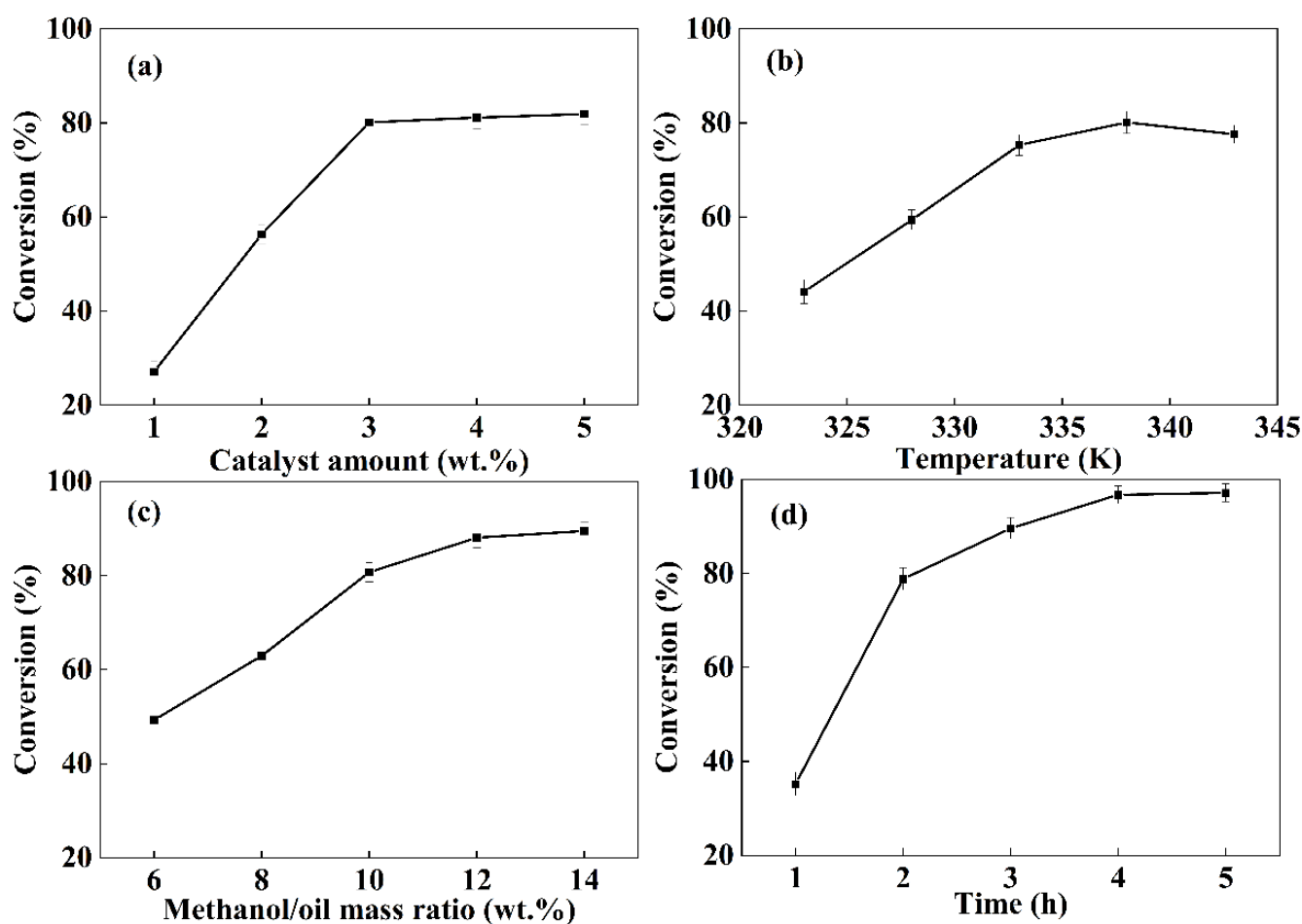
Figure 3. Influence of (**a**) catalyst amount, (**b**) temperature, (**c**) methanol/oil molar ratio and (**d**) reaction time on the conversion of jatropha oil by CaNa/AC.

Moreover, the stability of the catalyst at different transesterification temperatures was investigated by analyzing the basicity of the used catalyst in the temperature ranges. In the reaction temperature range of 323–338 K, there was a slight loss in the basicity of the used catalyst compared to that of the fresh sample, as shown in Figure 4. However, the basicity loss was up to 30% at 343 K, indicating the formation of a homogenous catalyst [52]. Furthermore, the gas bubbles were observed to continually appear and burst on the surface of the catalyst in the reaction when the temperature was 343 K, Therefore, it could be deduced that this perturbing activity induced the dissociation of active sites from CaNa/AC. These results indicated that the optimal temperature for transesterification was 343 K (within the range of this study).

Excess methanol is required to push the reaction toward the formation of FAME [53]. The methanol/oil molar ratio is commonly 6 for transesterification using a homogeneous base catalyst [54]. The reaction was performed with methanol/oil molar ratios ranging from 6:1 to 14:1 to investigate the effect of the methanol/oil ratio on the transesterification by CaNa/AC. The results in Figure 3c suggested that the conversion rate increased considerably with the increase in methanol/oil molar ratio, and the efficiency reached 88% at a 12:1 methanol/oil molar ratio. However, raising the methanol/oil molar ratio beyond 12:1 did not result in a significant promotion of the reaction rate. In conclusion, a methanol/oil molar ratio of 12:1 was deemed optimal.
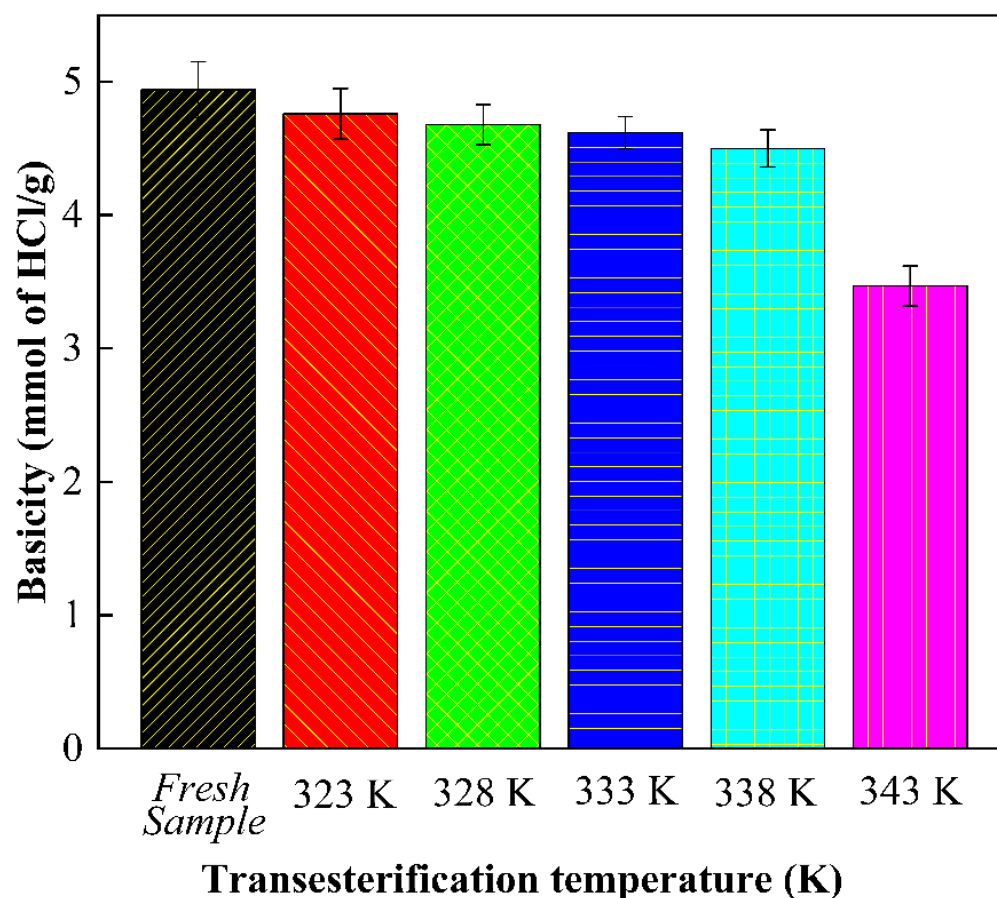
Figure 4. The basicity of used CaNa/AC at different temperatures.

The dependence of biodiesel formation on the reaction time range of 1 to 5 h is shown in Figure 3d, which indicated that the conversion increased significantly with increasing reaction time until 4 h, and a 97% yield was observed. Further increasing the reaction time did not affect the conversion, indicating the complete conversion. Therefore, the optimum reaction time of 4 h was selected for further studies.

3.7. Kinetic Analysis

Figure 5 shows Jatropha oil conversion variation with time at different temperatures in a methanol/oil mole ratio of 12:1, using 3 wt.% CaNa/AC to oil. The excess amount of methanol is generally used in order to increase the rate of the reaction and displace the equilibrium toward the products. Under this condition, researchers often ignored the intermediate reactions or assumed that the transformation of intermediates occurs rapidly [55]. As a result, most kinetic investigations of vegetable oil methanolysis and ethanolysis have been focused on the entire process [56]. Therefore, the reaction rate expression of the transesterification of Jatropha oil and methanol can be written in as Equation (1):

$$r = -dC_A/dt = kC_A^{\alpha}C_B^{\beta} \tag{1}$$

where k is the rate constant; C_A and C_B represent the concentration of Jatropha oil and methanol, respectively. α and β are the orders of reactants. The kinetic model is based on the overall reaction, and C_A can be calculated by taking x as the Jatropha oil conversion and C_A as the initial concentration of Jatropha oil. Due to a significant surplus of methanol in the reaction mixture, the concentration of methanol in transesterification can be safely

considered as constant. Thus, the reaction order of methanol is zero order. Therefore, Equation (1) can be simplified as Equation (2):

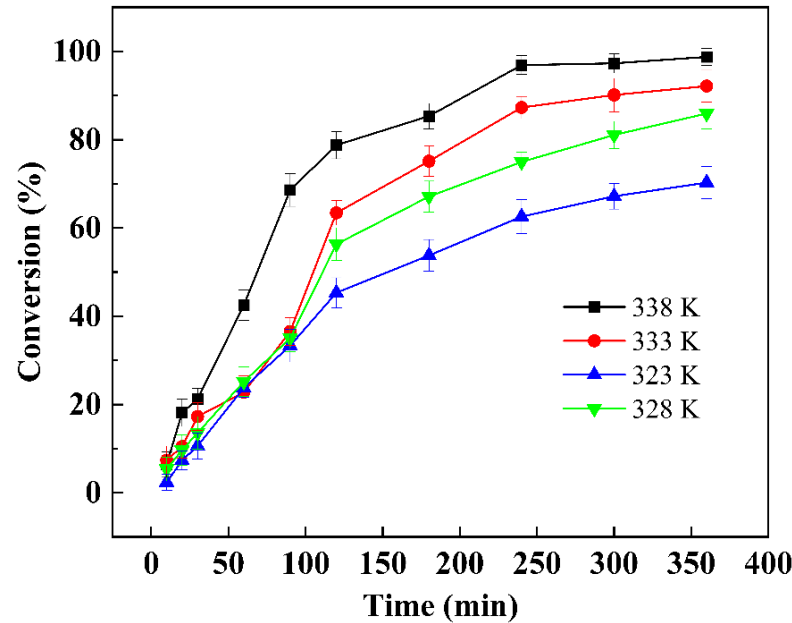$$r = -dC_A/dt = kC_A^n \tag{2}$$

Figure 5. Jatropha oil conversion variation of CaNa/AC at different temperatures.

In order to determine the overall reaction orders *n*, Equation (2) can be expressed as Equation (3):

$$\lg r = \lg(-dC_A/dt) = \lg k + n \lg C_A \tag{3}$$

Thus, *n* and *k* are obtained through plotting $\lg(-dC_A/dt)$ vs. $\lg C_A$.

Meanwhile, the Arrhenius equation can be used to compute the reaction's activation energy as Equation (4):

$$\lg k = -\frac{E_a}{2.303RT} + A \tag{4}$$

where E_a is the activation energy, R is the gas constant, *T* is the absolute temperature, and A is a constant.

In Figure 6a, the plots of $\lg(-dC_A/dt)$ vs. $\lg C_A$ were acceptably represented by straight lines having slopes of close to 1 at the three temperatures, which indicated that the transesterification for Jatropha oil and methanol was approximately a first-order reaction in the temperature range of 323–338 K. The fitting results shown in Table 3 are consistent with the previous report [57]. The calculated rate constants were calculated as 0.012, 0.0076, 0.0053, and 0.0034 min^{-1} at 323, 328, 333, and 338 K, respectively. These results indicated that higher temperatures sped up the reaction and shortened the reaction time in order to obtain the highest product yield, implying that reaction temperature was an important component in the transesterification and total product yield.

It has been reported that the activation energies of base-catalyzed heterogeneous transesterification reactions were in the range of 38~83 kJ·mol^{-1} [58]. The apparent activation energy was 75.6 kJ·mol^{-1}, which was closed to the activation energies (73.7 kJ·mol^{-1}) for the transesterification of soybean oil catalyzed by CaO [59], as determined from the slope of the plot in Figure 6b.

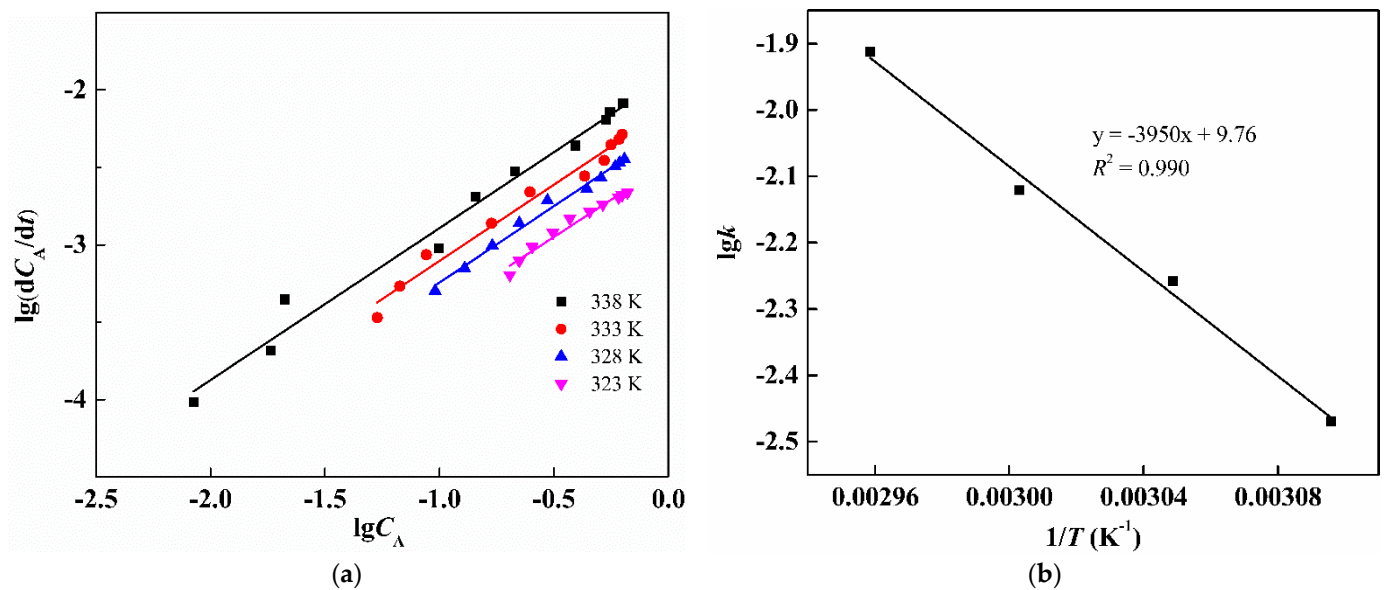**Figure 6.** Plots of (**a**) $\lg(-dC_A/dt)$ vs. $\lg C_A$ and (**b**) $\lg k$ vs. $1/T$ for the transesterification.

Table 3. The fitting results of $\lg(-dC_A/dt)$ vs. $\lg C_A$.

Temperature (K)	Slope	Intercept	R^2
323	0.961	−2.47	0.970
328	0.988	−2.26	0.989
333	0.985	−2.12	0.979
338	0.980	−1.91	0.982

3.8. Reusability of Catalyst

Reusability is an important criterion for a catalytic process affecting the process cost and economics [60,61]. Hence, the reusability of the catalysts was evaluated under identical reaction conditions. As shown in Figure 7, the oil conversion still remained above 80% after the fifth successive reuse of CaNa/AC. On the contrary, the oil conversion by Na/AC dramatically declined to 30% under the same conditions. The stability of a heterogeneous-based catalyst is critical because the bases leached during the transesterification reaction had a detrimental influence on the subsequent treatment of biodiesel substrates. The basicity loss of the catalyst was calculated by the basicity of the catalyst before and after the reaction. The results showed that the basicity losses were 30% and 6% for Na/AC and CaNa/AC, respectively, after the first transesterification. Therefore, the leached base from Na/AC could potentially act as a homogenous catalyst for transesterification, revealing a lack of chemical stability in this catalyst. In the case of the regenerated CaNa/AC, the catalytic activity decreased slightly compared to that of the fresh catalysts and still maintained an oil conversion of 80% after four cycles. These findings indicated that the introduction of calcium boosted the stability of the catalyst and enhanced its reusability, which is conducive for practical applications on large-scale operation.
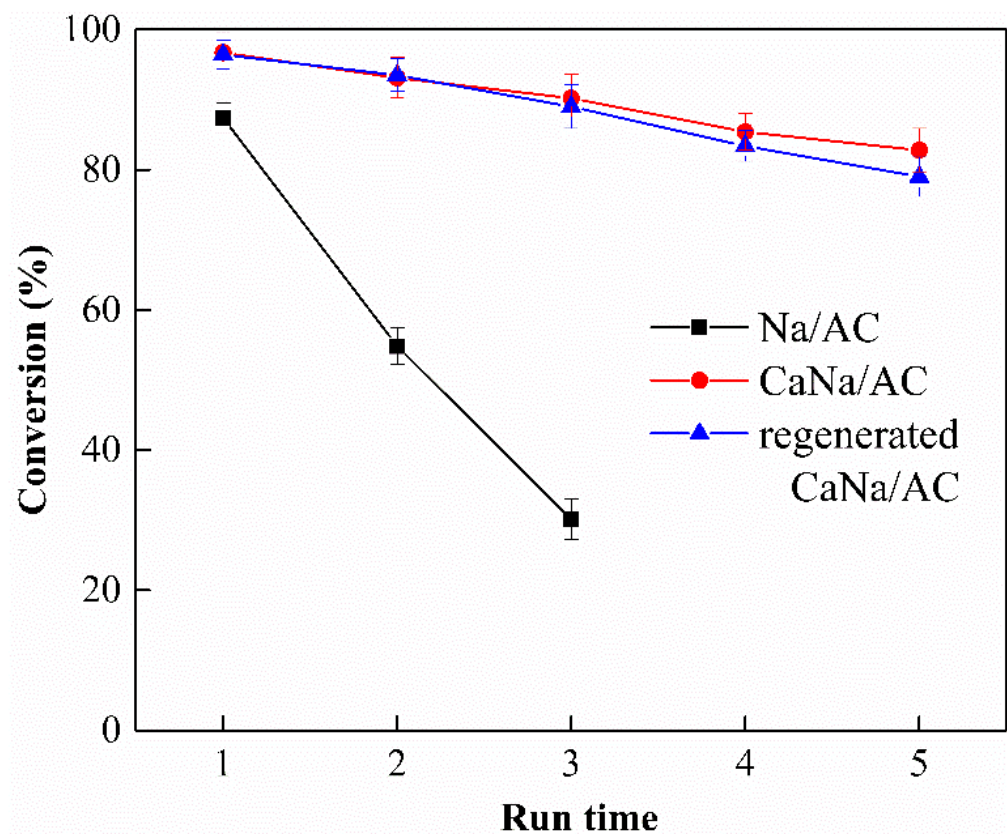
Figure 7. The reusability of Na/AC and CaNa/AC in the transesterification.

4. Discussion

CaNa/AC was successfully tested in the manufacture of biodiesel by transesterifying jatropha oil with methanol, and the kinetics parameters were determined by a differential. The reaction kinetics fitting results corresponded to a pseudo-first-order kinetic model and the rate constants at 323, 328, 333, and 338 K were 0.012, 0.0076, 0.0053, and 0.0033 min^{-1}, respectively, while the apparent activation energy was 75.6 kJ·mol^{-1}. As CaNa/AC showed high catalytic activity and economic properties, it could be deemed as a potential catalyst for biodiesel production.

In comparison to other catalyst preparation procedures (Table 4), the present strategy does not necessitate high-temperature roasting. CaNa/AC has an activity equivalent to other heterogeneous catalysts and can catalyze transesterification to yield biodiesel under extremely milder circumstances. In addition, alkaline bentonite catalysts were relatively cheap, and the preparation process was facile only using AC, calcium hydroxide, and sodium (or potassium) hydroxide without calcination. Hence, alkaline bentonite catalysts possess great prospects and cost-effectiveness for practical applications in biodiesel synthesis. Additionally, the further applications of this spent clay catalyst are currently underway in our laboratory such as reducing the free fatty acid content in raw oil due to its residual basicity, and then the waste clay derived from this deacidification could be used in road construction as a filler in the production of asphalts. This work will help to promote the practical application of this type of clay catalyst.

Table 4. Comparison of capacities of heterogeneous catalysts for biodiesel production.

Catalyst	Calcination Conditions	Transesterification Conditions				Conversion Rate (%)	References
		Catalyst Amount (wt.%)	Methanol/Oil Molar Ratio	Temperature (K)	Reaction Time (h)		
Na/SiO$_2$/TiO$_2$	773 K/5 h	9	20:1	343	2	97	[62]
KOH/Waste Ox bone	1173 K/3 h	5	12:1	338	4	97	[63]
LaTiO$_3$	973 K/3 h	5	4:1	353	1	90	[64]
Treated carbon nitrides	943 K/3 h	5	24:1	423	3	96	[65]
Acai seed ash	1073 K/4 h	12	18:1	373	1	98	[66]
K$^+$ trapped clay nanotubes	573 K/4 h	6	15:1	363	4	98	[67]
Copper modified montmorillonite clay	773 K/4 h	4	15:1	423	5	89	[68]
Marble waste powder	1123 K/2 h	7	16:1	338	3	95	[69]
CaNa/AC	**473 K/2 h**	**3**	**12:1**	**338**	**4**	**97**	**This study**

5. Conclusions

In summary, CaNa/AC was fabricated by modifying AC with Ca(OH)$_2$ and NaOH, and was, in turn, applied in the transesterification of Jatropha oil and methanol for the production of biodiesel. XRD, FT-IR, BET surface area, and CO$_2$-TPD characterizations revealed that Ca incorporation significantly enhanced the stability and recycling performance of the catalyst, and protected the acid centers on AC. In addition, Na ions incorporation mainly enhanced the base strength and basicity of the catalyst, resulting in higher biodiesel productions and faster reaction kinetics. Consequently, CaNa/AC achieved a fascinatingly higher oil conversion in the transesterification reaction (97%) under the optimal reaction conditions (3 wt.% catalyst amount, reaction temperature of 338 K, methanol/oil molar ratio of 12:1, and reaction time of 4 h). The conversion remained above 80% after five successive reuses of CaNa/AC, confirming its ultra-high stability during the transesterification reaction of Jatropha oil with methanol. Endorsing the high stability, cost-effectiveness, ease of synthesis, and ultra-high efficiency, the novelty CaNa/AC could be envisioned as an excellent catalyst for biodiesel generation on large-scale operation.

Author Contributions: Conceptualization, Y.W., X.H. and H.Z.; methodology, S.Y.; software, T.F.; formal analysis, K.L. and H.Z.; investigation, S.Y. and T.F.; writing—original draft preparation, Y.W. and X.H.; writing—review and editing, Y.W., Y.M. and H.Z.; project administration, Z.T. All authors have read and agreed to the published version of the manuscript.

Institutional Review Board Statement: Not applicable.

Informed Consent Statement: Not applicable.

Data Availability Statement: Data are within the article.

Conflicts of Interest: The authors declare no conflict of interest. The funders had no role in the design of the study; in the collection, analyses, or interpretation of data; in the writing of the manuscript, or in the decision to publish the results.

References

1. Bento, H.B.S.; Reis, C.E.R.; Cunha, P.G.; Carvalho, A.K.F.; De Castro, H.F. One-pot fungal biomass-to-biodiesel process: Influence of the molar ratio and the concentration of acid heterogenous catalyst on reaction yield and costs. *Fuels* **2021**, *300*, 120968. [CrossRef]
2. Dhawan, M.S.; Barton, S.C.; Yadav, G.D. Interesterification of triglycerides with methyl acetate for the co-production biodiesel and triacetin using hydrotalcite as a heterogenous base catalyst. *Catal. Today* **2021**, *375*, 101–111. [CrossRef]
3. Moraes, P.S.; Engelmann, J.I.; Igansi, A.V.; Sant Anna Cadaval, T.R., Jr.; Antonio De Almeida Pinto, L. Nile tilapia industrialization waste: Evaluation of the yield, quality and cost of the biodiesel production process. *J. Clean. Prod.* **2021**, *287*, 125041. [CrossRef]
4. Lourenço, V.A.; Nadaleti, W.C.; Vieira, B.M.; Li, H. Investigation of ethyl biodiesel via transesterification of rice bran oil: Bioenergy from residual biomass in Pelotas, Rio Grande do Sul-Brazil. *Renew. Sust. Energ. Rev.* **2021**, *144*, 111016. [CrossRef]
5. Aronica, L.A.; Albano, G. Supported Metal Catalysts for the Synthesis of N-Heterocycles. *Catalysts* **2022**, *12*, 68. [CrossRef]
6. Fechete, I.; Wang, Y.; Védrine, J.C. The past, present and future of heterogeneous catalysis. *Catal. Today* **2012**, *189*, 2–27. [CrossRef]
7. Lee, A.F.; Bennett, J.A.; Manayil, J.C.; Wilson, K. Heterogeneous catalysis for sustainable biodiesel production via esterification and transesterification. *Chem. Soc. Rev.* **2014**, *43*, 7887–7916. [CrossRef]
8. Rahman, N.J.A.; Ramli, A.; Jumbri, K.; Uemura, Y. Tailoring the surface area and the acid-base properties of ZrO_2 for biodiesel production from *Nannochloropsis* sp. *Sci. Rep.* **2019**, *9*, 16223. [CrossRef]
9. Lee, J.H.; Jeon, H.; Park, J.T.; Kim, J.H. Synthesis of hierarchical flower-shaped hollow MgO microspheres via ethylene-glycol-mediated process as a base heterogeneous catalyst for transesterification for biodiesel production. *Biomass Bioenergy* **2020**, *142*, 105788. [CrossRef]
10. Saman, S.; Balouch, A.; Talpur, F.N.; Memon, A.A.; Mousavi, B.M.; Verpoort, F. Green synthesis of MgO nanocatalyst by usingZiziphus mauritiana leaves and seeds for biodiesel production. *Appl. Organomet. Chem.* **2021**, *35*, e6199. [CrossRef]
11. Peixoto, A.F.; Soliman, M.M.A.; Pinto, T.V.; Silva, S.M.; Costa, P.; Alegria, E.C.B.A.; Freire, C. Highly active organosulfonic aryl-silica nanoparticles as efficient catalysts for biomass derived biodiesel and fuel additives. *Biomass Bioenergy* **2021**, *145*, 105936. [CrossRef]
12. Đặng, T.; Nguyễn, X.; Chou, C.; Chen, B. Preparation of cancrinite-type zeolite from diatomaceous earth as transesterification catalysts for biodiesel production. *Renew. Energy* **2021**, *174*, 347–358. [CrossRef]
13. Abukhadra, M.R.; Ibrahim, S.M.; Yakout, S.M.; El-Zaidy, M.E.; Abdeltawab, A.A. Synthesis of Na^+ trapped bentonite/zeolite-P composite as a novel catalyst for effective production of biodiesel from palm oil; Effect of ultrasonic irradiation and mechanism. *Energ. Convers. Manag.* **2019**, *196*, 739–750. [CrossRef]
14. Đặng, T.; Chen, B.; Lee, D. Optimization of biodiesel production from transesterification of triolein using zeolite LTA catalysts synthesized from kaolin clay. *J. Taiwan Inst. Chem. E* **2017**, *79*, 14–22. [CrossRef]
15. Da Costa, J.M.; de Andrade Lima, L.R.P. Transesterification of cotton oil with ethanol for biodiesel using a KF/bentonite solid catalyst. *Fuels* **2021**, *293*, 120446. [CrossRef]
16. Pawar, R.R.; Lalhmunsiama; Ingole, P.G.; Lee, S. Use of activated bentonite-alginate composite beads for efficient removal of toxic Cu^{2+} and Pb^{2+} ions from aquatic environment. *Int. J. Biol. Macromol.* **2020**, *164*, 3145–3154. [CrossRef]
17. Gozali Balkanloo, P.; Mahmoudian, M.; Hosseinzadeh, M.T. A comparative study between MMT-Fe_3O_4/PES, MMT-HBE/PES, and MMT-acid activated/PES mixed matrix membranes. *Chem. Eng. J.* **2020**, *396*, 125188. [CrossRef]
18. Funes, I.G.A.; Peralta, M.E.; Pettinari, G.R.; Carlos, L.; Parolo, M.E. Facile modification of montmorillonite by intercalation and grafting: The study of the binding mechanisms of a quaternary alkylammonium surfactant. *Appl. Clay Sci.* **2020**, *195*, 105738. [CrossRef]
19. Huang, G.; Song, Y.; Liu, C.; Yang, J.; Lu, J.; Liu, Z.; Liu, Z. Acid activated montmorillonite for gas-phase catalytic dehydration of monoethanolamine. *Appl. Clay Sci.* **2019**, *168*, 116–124. [CrossRef]
20. Boudissa, F.; Mirilà, D.; Arus, V.; Terkmani, T.; Semaan, S.; Proulx, M.; Nistor, I.; Roy, R.; Azzouz, A. Acid-treated clay catalysts for organic dye ozonation—Thorough mineralization through optimum catalyst basicity and hydrophilic character. *J. Hazard. Mater.* **2019**, *364*, 356–366. [CrossRef]
21. Bhatti, U.H.; Kazmi, W.W.; Muhammad, H.A.; Min, G.H.; Nam, S.C.; Baek, I.H. Practical and inexpensive acid-activated montmorillonite catalysts for energy-efficient CO_2 capture. *Green Chem.* **2020**, *22*, 6328–6333. [CrossRef]
22. Ayodele, O.B.; Abdullah, A.Z. Exploring kaolinite as dry methane reforming catalyst support: Influences of chemical activation, organic ligand functionalization and calcination temperature. *Appl. Catal. A Gen.* **2019**, *576*, 20–31. [CrossRef]
23. Saka, C.; Eygi, M.S.; Balbay, A. Cobalt loaded organic acid modified kaolin clay for the enhanced catalytic activity of hydrogen release via hydrolysis of sodium borohydride. *Int. J. Hydrog. Energy* **2021**, *46*, 3876–3886. [CrossRef]
24. Flessner, U.; Jones, D.J.; Rozière, J.; Zajac, J.; Storaro, L.; Lenarda, M.; Pavan, M.; Jiménez-López, A.; Rodríguez-Castellón, E.; Trombetta, M.; et al. A study of the surface acidity of acid-treated montmorillonite clay catalysts. *J. Mol. Catal. A Chem.* **2001**, *168*, 247–256. [CrossRef]
25. Wei, T.; Pan, Y.; Lu, G.; Tong, Z.; Xiao, H. Activated Clay Prepared by Waste Acid Recycling: Technology and Mechanism. *Environ. Eng. Sci.* **2010**, *27*, 531–535. [CrossRef]
26. Jeenpadiphat, S.; Tungasmita, D.N. Esterification of oleic acid and high acid content palm oil over an acid-activated bentonite catalyst. *Appl. Clay Sci.* **2014**, *87*, 272–277. [CrossRef]

27. Çakırca, E.E.; Akın, A.N. Study on heterogeneous catalysts from calcined Ca riched hydrotalcite like compounds for biodiesel production. *Sustain. Chem. Pharm.* **2021**, *20*, 100378. [CrossRef]

28. Singh, A.K.; Fernando, S.D. Preparation and Reaction Kinetics Studies of Na-based Mixed Metal Oxide for Transesterification. *Energ. Fuel.* **2009**, *23*, 5160–5164. [CrossRef]

29. Noiroj, K.; Intarapong, P.; Luengnaruemitchai, A.; Jai-In, S. A comparative study of KOH/Al_2O_3 and KOH/NaY catalysts for biodiesel production via transesterification from palm oil. *Renew. Energy* **2009**, *34*, 1145–1150. [CrossRef]

30. Rattanaphra, D.; Temrak, A.; Nuchdang, S.; Kingkam, W.; Puripunyavanich, V.; Thanapimmetha, A.; Saisriyoot, M.; Srinophakun, P. Catalytic behavior of La_2O_3-promoted $SO_4{}^{2-}/ZrO_2$ in the simultaneous esterification and transesterification of palm oil. *Energ. Rep.* **2021**, *7*, 5374–5385. [CrossRef]

31. Miladinović, M.R.; Krstić, J.B.; Zdujić, M.V.; Veselinović, L.M.; Veljović, D.N.; Banković-Ilić, I.B.; Stamenković, O.S.; Veljković, V.B. Transesterification of used cooking sunflower oil catalyzed by hazelnut shell ash. *Renew. Energy* **2022**, *183*, 103–113. [CrossRef]

32. Fang, X.; Xia, L.; Li, S.; Hong, Z.; Yang, M.; Xu, X.; Xu, J.; Wang, X. Superior 3DOM $Y_2Zr_2O_7$ supports for Ni to fabricate highly active and selective catalysts for CO_2 methanation. *Fuels* **2021**, *293*, 120460. [CrossRef]

33. Yaseen, M.; Ullah, M.; Subhan, S.; Ahmad, W.; Subhan, F.; Shakir, M. Recovery and characterization of useful benzene derivatives from spent engine oil through solvent extraction. *Chem. Eng. Res. Des.* **2021**, *175*, 51–60. [CrossRef]

34. Yaseen, M.; Ammara, O.; Ahmad, W.; Shakir, M.; Subhan, S.; Subhan, F.; Khan, K.; Iqbal, M.S. Preparation of titanium carbide reinforced polymer based composite nanofibers for enhanced humidity sensing. *Sens. Actuator A Phys.* **2021**, *332*, 113201. [CrossRef]

35. Tyagi, B.; Chudasama, C.D.; Jasra, R.V. Determination of structural modification in acid activated montmorillonite clay by FT-IR spectroscopy. *Spectrochim. Acta Part A Mol. Biomol. Spectrosc.* **2006**, *64*, 273–278. [CrossRef]

36. Lu, Y.; Zhang, Z.; Xu, Y.; Liu, Q.; Qian, G. CaFeAl mixed oxide derived heterogeneous catalysts for transesterification of soybean oil to biodiesel. *Bioresour. Technol.* **2015**, *190*, 438–441. [CrossRef]

37. Mashhadinezhad, M.; Shirini, F.; Mamaghani, M. Nanoporous Na^+-montmorillonite perchloric acid as an efficient heterogeneous catalyst for synthesis of merocyanine dyes based on isoxazolone and barbituric acid. *Microporous Mesoporous Mater.* **2018**, *262*, 269–282. [CrossRef]

38. Davoodbasha, M.; Pugazhendhi, A.; Kim, J.; Lee, S.; Nooruddin, T. Biodiesel production through transesterification of Chlorella vulgaris: Synthesis and characterization of CaO nanocatalyst. *Fuels* **2021**, *300*, 121018. [CrossRef]

39. Yaseen, M.; Khattak, S.; Ullah, S.; Subhan, F.; Ahmad, W.; Shakir, M.; Tong, Z. Oxidative desulfurization of model and real petroleum distillates using Cu or Ni impregnated banana peels derived activated carbon–NaClO catalyst–oxidant system. *Chem. Eng. Res. Des.* **2022**, *179*, 107–118. [CrossRef]

40. Subhan, S.; Yaseen, M.; Ahmad, B.; Tong, Z.; Subhan, F.; Ahmad, W.; Sahibzada, M. Fabrication of MnO_2 NPs incorporated UiO-66 for the green and efficient oxidative desulfurization and denitrogenation of fuel oils. *J. Environ. Chem. Eng.* **2021**, *9*, 105179. [CrossRef]

41. Krupskaya, V.; Novikova, L.; Tyupina, E.; Belousov, P.; Dorzhieva, O.; Zakusin, S.; Kim, K.; Roessner, F.; Badetti, E.; Brunelli, A.; et al. The influence of acid modification on the structure of montmorillonites and surface properties of bentonites. *Appl. Clay Sci.* **2019**, *172*, 1–10. [CrossRef]

42. Gajek, M.; Rapacz-Kmita, A.; Stodolak-Zych, E.; Zarzecka-Napierała, M.; Wilk, M.; Magdziarz, A.; Dudek, M. Microstructure and mechanical properties of diopside and anorthite glazes with high abrasion resistance. *Ceram. Int.* **2022**, *48*, 6792–6798. [CrossRef]

43. Tabrizi, S.H.; Tanhaei, B.; Ayati, A.; Ranjbari, S. Substantial improvement in the adsorption behavior of montmorillonite toward Tartrazine through hexadecylamine impregnation. *Environ. Res.* **2022**, *204*, 111965. [CrossRef]

44. Yang, G.; Deng, Y.; Ding, H.; Lin, Z.; Shao, Y.; Wang, Y. A facile approach to synthesize MCM-41 mesoporous materials from iron ore tailing: Influence of the synthesis conditions on the structural properties. *Appl. Clay Sci.* **2015**, *111*, 61–66. [CrossRef]

45. Muhammad, Y.; Rahman, A.U.; Rashid, H.U.; Sahibzada, M.; Subhan, S.; Tong, Z. Hydrodesulfurization of dibenzothiophene using Pd-promoted Co-Mo/Al_2O_3 and Ni-Mo/Al_2O_3 catalysts coupled with ionic liquids at ambient operating conditions. *RSC Adv.* **2019**, *9*, 10371–10385. [CrossRef]

46. Li, Z.; Ding, S.; Chen, C.; Qu, S.; Du, L.; Lu, J.; Ding, J. Recyclable Li/NaY zeolite as a heterogeneous alkaline catalyst for biodiesel production: Process optimization and kinetics study. *Energ. Convers. Manag.* **2019**, *192*, 335–345. [CrossRef]

47. Vishal, D.; Dubey, S.; Goyal, R.; Dwivedi, G.; Baredar, P.; Chhabra, M. Optimization of alkali-catalyzed transesterification of rubber oil for biodiesel production & its impact on engine performance. *Renew. Energy* **2020**, *158*, 167–180. [CrossRef]

48. Esonye, C.; Onukwuli, O.D.; Ofoefule, A.U. Chemical kinetics of a two-step transesterification of dyacrodes edulis seed oil using acid-alkali catalyst. *Chem. Eng. Res. Des.* **2019**, *145*, 245–257. [CrossRef]

49. Takase, M.; Zhang, M.; Feng, W.; Chen, Y.; Zhao, T.; Cobbina, S.J.; Yang, L.; Wu, X. Application of zirconia modified with KOH as heterogeneous solid base catalyst to new non-edible oil for biodiesel. *Energ. Convers. Manag.* **2014**, *80*, 117–125. [CrossRef]

50. Jung, S.; Kim, M.; Lin, K.A.; Park, Y.; Kwon, E.E. Biodiesel synthesis from bio-heavy oil through thermally induced transesterification. *J. Clean. Prod.* **2021**, *294*, 126347. [CrossRef]

51. Subhan, S.; Ur Rahman, A.; Yaseen, M.; Ur Rashid, H.; Ishaq, M.; Sahibzada, M.; Tong, Z. Ultra-fast and highly efficient catalytic oxidative desulfurization of dibenzothiophene at ambient temperature over low Mn loaded Co-Mo/Al_2O_3 and Ni-Mo/Al_2O_3 catalysts using NaClO as oxidant. *Fuels* **2019**, *237*, 793–805. [CrossRef]

52. Jayakumar, M.; Karmegam, N.; Gundupalli, M.P.; Bizuneh Gebeyehu, K.; Tessema Asfaw, B.; Chang, S.W.; Ravindran, B.; Kumar Awasthi, M. Heterogeneous base catalysts: Synthesis and application for biodiesel production—A review. *Bioresour. Technol.* **2021**, *331*, 125054. [CrossRef]

53. Ishak, N.; Estephane, J.; Dahdah, E.; Chalouhi, L.M.; Nassreddine, S.; El Khoury, B.; Aouad, S. Outstanding activity of a biodiesel coated K_2O/fumed silica catalyst in the transesterification reaction. *J. Environ. Chem. Eng.* **2021**, *9*, 104665. [CrossRef]

54. Hoque, M.E.; Singh, A.; Chuan, Y.L. Biodiesel from low cost feedstocks: The effects of process parameters on the biodiesel yield. *Biomass Bioenergy* **2011**, *35*, 1582–1587. [CrossRef]

55. Putra, M.D.; Irawan, C.; Udiantoro; Ristianingsih, Y.; Nata, I.F. A cleaner process for biodiesel production from waste cooking oil using waste materials as a heterogeneous catalyst and its kinetic study. *J. Clean. Prod.* **2018**, *195*, 1249–1258. [CrossRef]

56. Shahla, S.; Ngoh, G.C.; Yusoff, R. The evaluation of various kinetic models for base-catalyzed ethanolysis of palm oil. *Bioresour. Technol.* **2012**, *104*, 1–5. [CrossRef]

57. Li, E.; Xu, Z.P.; Rudolph, V. MgCoAl–LDH derived heterogeneous catalysts for the ethanol transesterification of canola oil to biodiesel. *Appl. Catal. B* **2009**, *88*, 42–49. [CrossRef]

58. Zięba, A.; Pacuła, A.; Drelinkiewicz, A. Transesterification of triglycerides with methanol catalyzed by heterogeneous zinc hydroxy nitrate catalyst. Evaluation of variables affecting the activity and stability of catalyst. *Energy Fuel.* **2010**, *24*, 634–645. [CrossRef]

59. Liu, X.; Piao, X.; Wang, Y.; Zhu, S. Model Study on Transesterification of Soybean Oil to Biodiesel with Methanol Using Solid Base Catalyst. *J. Phys. Chem. A* **2010**, *114*, 3750–3755. [CrossRef]

60. Yaseen, M.; Ullah, S.; Ahmad, W.; Subhan, S.; Subhan, F. Fabrication of Zn and Mn loaded activated carbon derived from corn cobs for the adsorptive desulfurization of model and real fuel oils. *Fuels* **2021**, *284*, 119102. [CrossRef]

61. Muhammad, Y.; Rashid, H.U.; Subhan, S.; Rahman, A.U.; Sahibzada, M.; Tong, Z. Boosting the hydrodesulfurization of dibenzothiophene efficiency of Mn decorated (Co/Ni)-Mo/Al_2O_3 catalysts at mild temperature and pressure by coupling with phosphonium based ionic liquids. *Chem. Eng. J.* **2019**, *375*, 121957. [CrossRef]

62. Khan, I.W.; Naeem, A.; Farooq, M.; Ghazi, Z.A.; Saeed, T.; Perveen, F.; Malik, T. Biodiesel production by valorizing waste non-edible wild olive oil using heterogeneous base catalyst: Process optimization and cost estimation. *Fuels* **2022**, *320*, 123828. [CrossRef]

63. Jayakumar, M.; Gebeyehu, K.B.; Selvakumar, K.V.; Parvathy, S.; Kim, W.; Karmegam, N. Waste Ox bone based heterogeneous catalyst synthesis, characterization, utilization and reaction kinetics of biodiesel generation from Jatropha curcas oil. *Chemosphere* **2022**, *288*, 132534. [CrossRef] [PubMed]

64. Rezania, S.; Mahdinia, S.; Oryani, B.; Cho, J.; Kwon, E.E.; Bozorgian, A.; Rashidi Nodeh, H.; Darajeh, N.; Mehranzamir, K. Biodiesel production from wild mustard (Sinapis Arvensis) seed oil using a novel heterogeneous catalyst of $LaTiO_3$ nanoparticles. *Fuels* **2022**, *307*, 121759. [CrossRef]

65. De Medeiros, T.V.; Macina, A.; Naccache, R. Graphitic carbon nitrides: Efficient heterogeneous catalysts for biodiesel production. *Nano Energy* **2020**, *78*, 105306. [CrossRef]

66. Mares, E.K.L.; Gonçalves, M.A.; Da Luz, P.T.S.; Da Rocha Filho, G.N.; Zamian, J.R.; Da Conceição, L.R.V. Acai seed ash as a novel basic heterogeneous catalyst for biodiesel synthesis: Optimization of the biodiesel production process. *Fuels* **2021**, *299*, 120887. [CrossRef]

67. Abukhadra, M.R.; Mostafa, M.; El-Sherbeeny, A.M.; Ahmed Soliman, A.T.; Abd Elgawad, A.E.E. Effective transformation of waste sunflower oil into biodiesel over novel K^+ trapped clay nanotubes (K^+/KNTs) as a heterogeneous catalyst; response surface studies. *Microporous Mesoporous Mater.* **2020**, *306*, 110465. [CrossRef]

68. Munir, M.; Ahmad, M.; Rehan, M.; Saeed, M.; Lam, S.S.; Nizami, A.S.; Waseem, A.; Sultana, S.; Zafar, M. Production of high quality biodiesel from novel non-edible Raphnus raphanistrum L. seed oil using copper modified montmorillonite clay catalyst. *Environ. Res.* **2021**, *193*, 110398. [CrossRef]

69. Bargole, S.S.; Singh, P.K.; George, S.; Saharan, V.K. Valorisation of low fatty acid content waste cooking oil into biodiesel through transesterification using a basic heterogeneous calcium-based catalyst. *Biomass Bioenergy* **2021**, *146*, 105984. [CrossRef]